J Mater Sci (2008) 43:2869–2878
DOI 10.1007/s10853-007-2085-9

Measurement of wet fiber flexibility by confocal laser scanning microscopy

Dongbo Yan · Kecheng Li

Received: 5 April 2007 / Accepted: 6 August 2007 / Published online: 25 September 2007

Abstract A new method for fiber flexibility measurement has been developed using confocal laser scanning microscopy (CLSM), based on the fiber conformability method. Freespan length was measured directly from the transverse view of the fiber span, so the accuracy of the measurement was greatly improved. The collapsibility and moment of inertia can also be measured from the fiber cross section obtained from CLSM. Thus, it was possible to measure the elastic modulus of individual fibers. Therefore, all the basic properties of fiber that affect its conformability, including fiber wall thickness, moment of inertia, and elastic modulus, can be measured within a single test. Results show that both fiber collapsibility and the elastic modulus of the fiber wall affect the fiber flexibility. Collapsibility is controlled mainly by fiber wall thickness. A refining or bleaching process can increase fiber flexibility mainly by altering fiber elastic modulus.

Introduction

The wet fiber flexibility is recognized as one of the most important and fundamental papermaking properties of pulp fibers. The fiber network structure in a paper sheet is directly affected by fiber flexibility during sheet consolidation. Flexible fibers are more conformable to one another, thus forming more contact area among fibers. Since it determines the total inter-fiber contact area and the voids in the fiber network, fiber flexibility plays a dominant role in determining most of the paper properties such as bulk, permeability, opacity, surface smoothness, and physical strengths. The fiber flexibility of mechanical pulp, such as bleached chemi-thermomechanical pulp (BCTMP) fibers, is more important when BCTMP fibers are used in wood-free fine paper grades to improve paper bulk and opacity [1]. Compared with chemical pulp fibers, which usually collapse completely during fiber processing, mechanical pulp fibers do not collapse or partially collapse depending on the papermaking process [2]. Collapsed fibers will have higher flexibility than the uncollapsed ones. Therefore, it is important to understand how the fiber collapsibility affects the fiber flexibility.

Several methods have been reported for individual fiber flexibility measurement [3–7]. Most of them are based on small deflection beam theory, by measuring the displacement of a fiber beam, while applying a transverse force or bending moment on the fiber. Assumed as a ideal elastic beam, the flexibility (F) of individual fibers is defined as the reciprocal of its bending stiffness, $F = 1/EI$, where E is the elastic modulus of fiber wall, and I is the moment of inertia of fiber cross section. Seborg and Simmonds [8] measured the stiffness of dry fibers by exerting a force on a fiber, using a quartz spring to bend it like a cantilever beam. The flexural stiffness EI is determined from the slope of load-deflection curve. James [9] calculated the fiber stiffness by measuring the resonance frequency of a fiber cantilever. Hydrodynamic or bending beam methods have also been developed for the fiber flexibility measurement by hydrodynamic forces generated by water flow and image analysis, so that individual fiber handling can be avoided. Fibers are supported in different ways. Samuelsson [3] used a mechanical jaw to clamp the fibers. Tam

D. Yan · K. Li (✉)
Department of Chemical Engineering, Limerick Pulp and Paper Research and Education Centre, University of New Brunswick, Fredericton, NB, Canada E3B 6C2
e-mail: kecheng@unb.ca

Doo and Kerekes [10] supported the fiber on one end of a capillary tube, so that mechanical damage to the fiber can be avoided. Kuhn et al. [6] developed a device that bends fibers by a T-junction tube when fibers in water flow out of a capillary. The fiber deformation is observed by a microscope, and the force is calculated according to hydrodynamic theory. The conformability testing is another typical method for fiber flexibility measurement. This method is first proposed by Mohlin [4], and then further developed by Steadman and Luner [7]. In the method, fibers are wet pressed onto a thin wire that is fixed on a glass slide and arcs over it. The non-contact span, or freespan length of the fiber is determined to calculate the fiber flexibility according to the beam deflection theory. Since only a conventional light microscope is required, and it can provide a numerical measure in an engineering unit, this method has commonly been used for fiber flexibility measurement [11–13].

However, in the Steadman method, a wire of 25 μm diameter was used as the support wire for forming the fiber arc over it. A larger wire will lead to a large arc, which will be easier to identify with a conventional microscope, but a large wire will also increase the deflection ratio. Lawryshyn and Kuhn [14] found that a large deflection ratio will introduce errors in the calculated flexibility results since all the fiber flexibility measurement methods are based on the small deflection beam theory. Rob et al. [15] proposed a method in which a real fiber is used as support instead of a metal wire. This reduces the deflection height substantially, and more importantly, it simulates the real fiber-fiber interaction in a paper sheet. However, it is impossible to use the conventional microscopical technique to measure the deflection height. In doing so, they developed a sophisticated technique based on counting the interference fringes formed in the non-contact area between the fiber and the glass slide.

Confocal Laser Scanning Microscope (CLSM) is a technique, originally developed for rapid and nondestructive three-dimensional imaging of living cells. In recent years, it has been used increasingly in the pulp and paper research, e.g., imaging fiber cross sections and evaluating fiber collapse behavior [16–19] , paper cross section analysis [20], and chemical distribution across the fiber wall [21]. The optical sectioning function makes CSLM an ideal tool for directly observing the shape of the deformed fiber from the transverse view, and the fiber cross-sectional geometry with higher accuracy. The shape of the deformed fiber over another fiber not only reveals the nature of fiber–fiber interaction, but also reveals the nature of fiber deformation; i.e., shear deformation versus bending deformation, as proposed by Waterhouse and Page [22]. Observation of the fiber cross-sectional geometry provides opportunity for calculating the movement of inertia, and in turn, the elastic modulus of the fiber wall.

This article discusses a new technique for fiber flexibility measurement by using CLSM, based on the conformability method developed by Steadman and Luner [7]. With CLSM, not only the fiber flexibility, but also the nature of fiber deformation, fiber elastic modulus, and the fiber collapsibility can be determined. Therefore, the CLSM method can also lead to a new insight into how the fiber wall modulus and fiber collapsibility are altered in the pulping and papermaking processes, and how they affect the fiber flexibility.

Experimental

Materials and sample preparation

Four commercial pulps, bleached spruce kraft pulp (BKP), aspen CTMP, aspen BCTMP, and birch BCTMP, were obtained from two Canadian paper mills. Aspen CTMP, aspen BCTMP are taken from the same production line. The aspen BCTMP were further refined by a PFI mill at 4% consistency to 3,000 revolutions and at 10% consistency to 4,000 revolutions denoted as LCR, and MCR, respectively. The CSF freeness of LCR and MCR are 236 mL and 268 mL, respectively.

Acetone washed glass fibers were deposited on glass slides (Fisher brand precleaned microscope slide) as support wires, prior to depositing pulp fibers on them. Glass fibers (0.5 g, CDS Analytical 1001-0345) are suspended in 1 L of distilled water and drained onto a piece of filter paper (Fisher brand Q8) by a TAPPI standard handsheet former. The suspension was swirled before draining so that it was spinning while draining down, thus glass fibers oriented approximately in parallel close to the edge of the filter paper. Then the glass fibers were transferred onto microscope slides by placing and gently tapping the filter paper onto the slides.

To enhance the fluorescence intensity, pulp fibers (0.3 g o.d) were stained in 20 mL 0.1% Safranin-O for 24 h at room temperature, and then diluted to 0.03% consistency and drained onto a filter paper in the same manner, as it was done for the glass fibers. The filter paper with fibers is placed on two pieces of dry blotting paper, and is then pressed onto eight glass slides at 340 kPa by a standard handsheet press (Labtech) for 5 min. Prior to pressing, the glass slide and the filter paper were arranged in a way such that the pulp fibers and the glass fibers cross each other perpendicularly. The actual pressures on fiber samples are calculated based on the projected fiber area. Slides are dried in air and kept under TAPPI standard conditions before CLSM imaging. It should be noted that not all the fibers cross each other perpendicularly. A pulp fiber was measured only when the angle was within

90 ± 10°. About 30–50% of fibers form almost perpendicular crossings. Since there are about a thousand pulp fibers on a single glass slide, sufficient perfect crossings can be found.

CLSM methodology

CLSM operation

Image scanning was carried out with a Leica TCS-SP2 confocal laser scanning microscope. A dry objective lens (HC FLOUTAR 50 ×) with a numerical aperture of 0.8 is used for imaging transverse and cross section of fibers that were wet pressed on a glass slide. An excitation wavelength of 514 nm from an Ar laser is used. The pinhole size is set at the optimum value by Leica Confocal Control software. The emission light collected by detector (PMT) is set from 525 to 760 nm. The gain and offset of PMT are adjusted automatically for each fiber by the software to ensure a constant image quality. The CLSM is operated in *XZ* scanning mode to obtain both transverse and cross-sectional image. Scanning step size in *Z* direction is 0.12 μm. An oil immersion lens (HCX OLAPO CS 63 × 1.4) was used for imaging fiber cross section before wet pressing.

Image modes

The basic imaging mode of CLSM is an *XY* plane, or section of the sample of the focal plane. The major difference between CLSM and conventional light microscope (LM) is that CLSM allows only the signals from the focal plane to be recorded, so the image formed is only a plane, not the entire sample object, while in LM, signals from above and below the focal plane can be recorded. Therefore, the CLSM image is crisper, and is of higher resolution. By changing the focal plane along the height direction, a series of focal planes, also called optical sections, can be imaged as shown in Fig. 1a. With the software, these optical sections can be stacked up to construct a 3D image of the object, as shown in Fig. 1b. It is apparent that with the 3D image, the freespan length (L_1 and L_2), and the deflection height (d) can be easily determined. In addition, the shape or the nature of the fiber deformation can be revealed.

Similarly, CLSM can also scan a single line through the fibers, thickness in either an *XZ* plane or *YZ* plane, as shown in Fig. 2. From *XZ* plane, the transverse view of the fiber deformation can be obtained, which provides the same information as the 3D image, and from the *YZ* plane, the cross-sectional view of the fiber can be obtained, which can

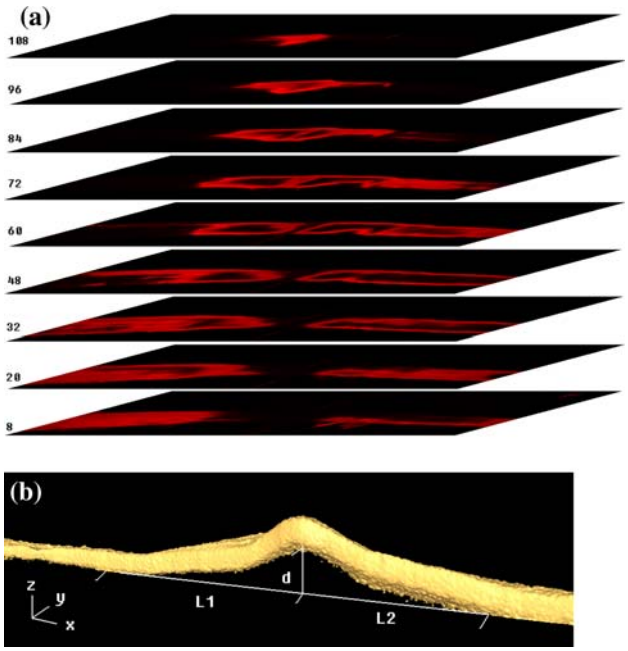

Fig. 1 CLSM images of an aspen BCTMP fiber bending over a glass wire. (**a**) Images of a series of XY sections; (**b**) A 3D images of the fiber reconstructed from the series of XY sections shown in (**a**)

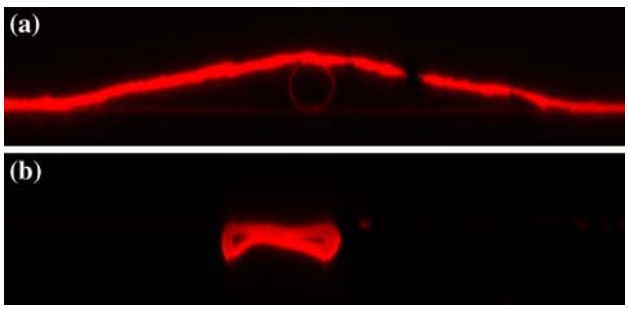

Fig. 2 Transverse and cross sectional views obtained with CLSM scanning through (**a**) *XZ* plane and (**b**) *YZ* plane

be used to determine the collapsibility of the fiber and the moment of inertia of the fiber wall. In this experiment, the single line scan is used, since it takes much less time than the series of focal planes.

Image processing

To improve the accuracy of the measurement, and avoid subjective errors, image processing is performed with the image processing toolbox in Matlab 7.0 (Mathworks Inc.). CLSM images are smoothed using lowpass filtering, and then converted into binary format (Fig. 3). The threshold for binarization was determined automatically by the double peak histogram method [23, 24]. All measurements were carried out on the binarized images.

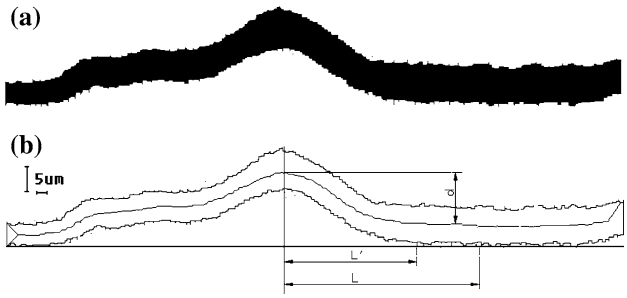

Fig. 3 Binarized image of the transverse view of a BCTMP fiber (**a**), and defining a neutral bending plane for freespan length and deflection height measurement (**b**)

Freespan length (L) *and deflection height* (d)

Since the fiber thickness is not uniform along the fiber length, and a fiber does not collapse uniformly along the fiber length, the thickness of the fiber cross-section may affect the deflection height and freespan length. In this experiment, a neutral bending plane is defined as the symmetric center in fiber thickness along the fiber length (Fig. 3). The neutral bending plane is located by applying skeletonization operation to the fiber transverse images [25]. Since fiber edges on the binarized image are usually not smooth, several "open" operations are required before skeletonization, so that the object can be smoothed and isolated pixels are removed. The deflection height d is defined as the vertical distance between the highest and the lowest pixels on the neutral bending plane. The freespan length L is defined as the horizontal distance between the highest pixel and the lowest pixel at the origin of horizontal segment of the neutral bending plane.

Fiber collapsibility (AR) *and moment of inertia* (I)

Fiber collapsibility was measured as the aspect ratio of the fiber cross-section dimension according to Jang [26].

$$AR = \frac{D_{\min}}{D_{\max}} \tag{1}$$

where $D_{\min}$ is the fiber thickness (shortest Feret diameter), and $D_{\max}$ is the fiber width (longest Feret diameter), which were obtained from a binarized fiber cross-sectional image (Fig. 4). The cross-sectional images were taken from the fiber on the top of the support wire. The main reason that this portion of the fiber was chosen for collapsibility measurement is that this portion of the fiber was subjected to the maxima stress, and it is consistent if the same spot was chosen for all the fibers measured throughout the experiment. In theory, the cross section could be extracted from part of the free-span region, but not the part, which is

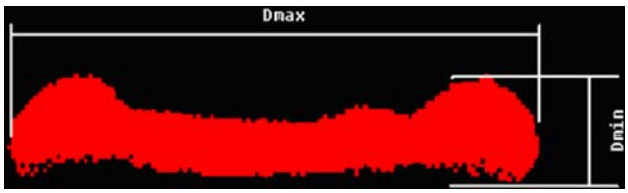

Fig. 4 Typical binarized cross-sectional image of an collapsed aspen BCTMP fiber, and the measurement of the cross sectional demensions

in contact with the glass slide, since the part in contact with the glass slide may not contribute much to the deformation process of the fiber under stress.

It is because of the irregular shape of the fiber cross section, that the moment of inertia (I) of fiber with regard to the neutral bending plane was calculated on the basis of relative location of each pixel (Eq. 2) [27].

$$I = \sum I_{\mathrm{i}} = \sum \left(\frac{ab^3}{12} + A_{\mathrm{i}} x^2 \right) \tag{2}$$

where a and b is the width and height of the pixel. A_{i} is the area of a pixel and x is the distance of pixel i to the neutral bending plane. The fiber wall thickness was only measured on the fibers without wet pressing from the fiber cross-sectional images following Jang's procedure [17, 28].

Results

Typical images of the transverse view of the fiber deformation acquired with CLSM *XZ* scanning mode are shown in Fig. 2a. From these images, fiber deformation height and free-span length are measured. Fiber flexibility was calculated on the basis of Steadman and Luner method [7] by assuming that the fibers are subjected to only pure bending.

$$\text{Flexibility} = \frac{1}{EI} = \frac{72d}{qL^4} \tag{3}$$

where E and I is the elastic modulus and the moment of inertia of the fiber wall, respectively; d is the deflection height, L is the free span length, and q is the pressing load on the fiber in N/m.

It was observed that almost all BKP fibers were collapsed, and solid fiber walls are imaged (Fig. 5a). In contrast, mechanical pulp fibers were not completely collapsed, which can be seen from the lumen area appearing dark between the fiber walls (Fig. 5b). The shapes of the deformation of the two types of fibers were also distinguishable. The shape of the deformation of the BKP fibers appeared straight, resembling a shear deformation, but that of the BCTMP appeared more like a bending deformation. This confirms Waterhouse and Pages's finding [22] that

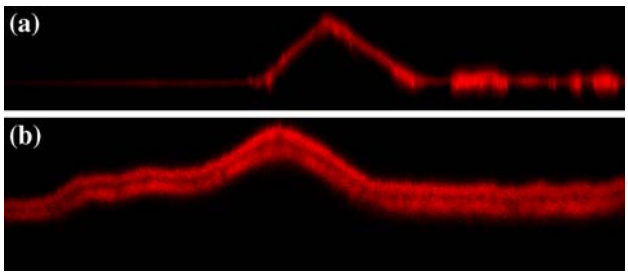

Fig. 5 A XZ transverse views of fibers wet pressed on a 10 μm diameter glass fiber at 340 kPa for 5 min. Imaged in X–Z–Y scanning mode, 50 × dry lens. Image size 300 × 31.5 μm (width × height). (**a**) spruce BKP (**b**) aspen BCTMP

shear contribution can be substantial in the Steadman and Luner method. In this article, only bending deformation is considered on the basis of Steadman and Luner method. To limit the shear contribution and make the results comparable to other hardwood pulp fibers, the pressure used for BKP fibers was reduced to 220 kPa,, and the resultant deflection ratio of the same was about 20%, close to that of hardwood pulp samples.

Various types of pulp fibers were measured using the method. About 40–50 fibers of each pulp sample were measured. It can be seen from Table 1, that the deflection ratios, which are the ratios of the deflections in fiber thickness direction to the free span lengths, are about 20% or below. According to Lawryshyn and Kuhn [14], when the small deflection theory is used, as in the Steadman method, the error introduced can be controlled to about 5% for the deflection ration less than 20%. Due to the heterogeneity of pulp fibers, the flexibility values of each pulp distribute in a wide range (Fig. 6). Therefore, the median value of flexibility for each sample is presented in Table 1. The measured flexibility values of each pulp sample were also compared using analysis of variance test (One-way ANOVA) with SPSS (SPSS Inc., USA). The significance between any two samples is less than 0.001, which indicates that this method is able to differentiate different types of fibers effectively with a sample size of about 50.

Discussion

Freespan length by CLSM and LM

An advantage of using CLSM is that CLSM can accurately identify the physical contact points from the transverse view of the fiber span, and hence the exact freespan length can be measured. With introducing the concept of "neutral bending plane" as discussed foregoing, the accuracy of the freespan length measured is even greater. Another advantage is that the deflection height can be measured directly, other than being assumed to be the diameter of the support wire. As reported by Rob et al. [15], in some cases the overlaying fiber may conform to the support fiber by overlapping. Figure 7a illustrates the difference in measured freespan length by CLSM and LM for a perfect span shape. It is due to light interference between the glass slide and the fiber that, LM is only able to identify the optical contact points, so the measured freespan length is *"L′"* as compared to the *"L"* measured with CLSM.

Table 2 shows the difference in the average freespan length measured with CLSM and LM (Leica DM4500 microscope). For thick-walled and partially collapsed fibers (BCTMP and CTMP), the freespan measured by CLSM (L) is up to 35% larger. However, for flexible and thin-walled fibers, the freespan measured with LM is greater than that measured with CLSM. According to the illustration in Fig. 7a, L is always larger than $\acute{L}$, but this is only for a perfect deformation shape. In reality, fibers do not always deform like that, and the deformation is not symmetrical about the central point or the support wire, as shown in Fig. 5b and 7b. This is probably due to the non-uniformity of fiber wall structure. With CLSM, only the perfect deformation on the right side is measured since the shape can be seen. With LM, the freespan lengths of both sides are measured with out seeing the deformation shape. In some cases, as shown in Fig. 7b, the first contact point (A) can be missed due to irregular deformation shape, and the second contact point (B) is taken as the contact point, thus, the left half OB is much larger than the real freespan OA. It was observed in this experiment that about 50% BCTMP

Table 1 Median values of the fiber flexibility of various types of fibers by CLSM

Pulp Sample Type	No. of Fibers measured	Freespan length (μm)	Support glass rod diameter (μm)	Deflection ratio (%)	Flexibility × 10^{-11} (N^{-1} m^{-2})
Spruce BKP*	31	59.28	12.8	21.59	73.7
Aspen BCTMP	52	67.83	12.41	18.30	14.78
Aspen CTMP	44	160.05	12.11	7.57	0.74
Birch CTMP	74	192.48	12.80	6.65	0.78
Birch BCTMP	40	128.94	15.29	11.86	2.94
LCR	42	51.85	9.96	19.21	38.97
MCR	52	43.63	9.77	22.39	54.69

* Pressed at 220 kPa

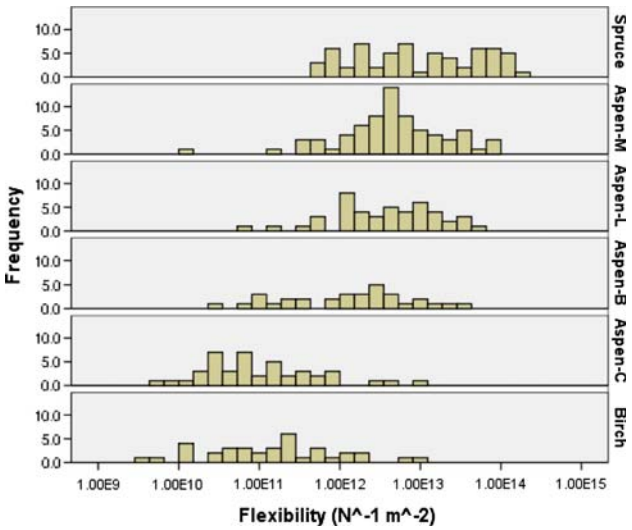

Fig. 6 Distribution of measured flexibility values of individual fibers. Spruce: spruce BKP; Aspen-M: MCR; Aspen-L: LCR; Aspen-B: aspen BCTMP; Aspen-C: aspen CTMP; Birch: birch BCTMP

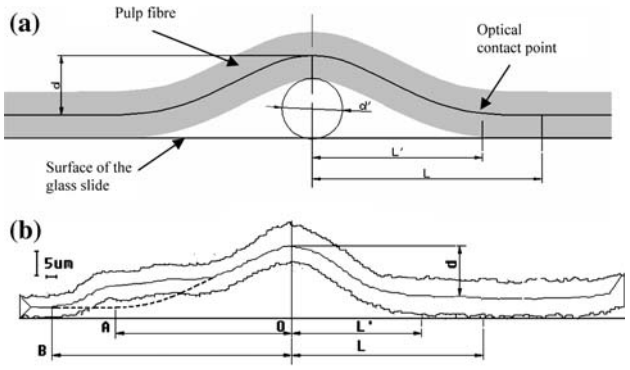

Fig. 7 Measurement of the freespan length by CLSM and LM. (**a**) a perfect bending shape, and (**b**) non-symmetrical bending. *L′*—free span length measured with a LM, *L*—free span length measured with a CLSM and image processing

fibers formed irregular deformation; only perfect span shape was measured for calculating the fiber flexibility. The rationale behind is, that if irregular deformation is formed, it means that the operation or the result does not comply with the beam deflection theory, so the measurement or calculation would be invalid. This is another benefit of using CLSM. A light microscope cannot identify the irregular shape, so all kinds of deformation were measured, which lead to errors in the measurements.

Fiber collapsibility and moment of inertia

Since CLSM can image the fiber cross section directly, the collapsibility and the moment of inertia can be obtained, when the fiber flexibility is measured. Therefore, additional information on how the fiber collapsibility affects the fiber flexibility can be revealed. Figure 8 shows typical cross section images of fibers obtained with CLSM. Thin-walled spruce BKP fibers collapsed completely without wet pressing (Fig. 8a). The thick walled mechanical fiber (birch BCTMP fibers) collapse slightly after pressing. Originally, there was a partial collapse in BCTMP fibers the wet pressing (Fig. 8d). After pressing, they collapsed almost completely (Fig. 8e). The aspect ratios (*AR*) listed in Table 3 give quantitative information of the collapsibility of the different types of fibers during flexibility measurement.

Once fibers collapse, the thickness of the fiber cross sections reduce greatly, thus, reducing the moment of inertia of the fiber. Therefore, the collapsibility of fibers affects the flexibility of the fibers by reducing the moment of inertia. Figure 9 shows the relationship between fiber moment of inertia and the fiber collapsibility. When the fiber collapsibility is small, as for the BCTMP fibers, a small change of fiber collapsibility can cause significant change in fiber moment of inertia. It can also be seen in Table 3, that both bleaching and refining significantly increased the fiber collapsibility of aspen fibers.

It can be seen from Fig. 10 that the fiber collapsibility is essentially determined by the fiber wall thickness. Thin-walled BKP fibers collapse completely without any wet

Table 2 Comparison of freespan length and deflection height measurement by CLSM and conventional light microscope (LM)

Fiber Type	Mean Fiber thickness (μm)	Median value of Freespan length at neutral bending plane (μm ± SD)	Measured freespan length with LM (μm ± SD)	Relative difference of measured freespan length between CLSM and LM (%)
Aspen CTMP	7.62 ± 1.86	160.05 ± 61.61	103.10 ± 61.01	–35.58
Birch BCTMP	10.35 ± 3.81	128.94 ± 41.44	86.56 ± 56.83	–32.89
Aspen BCTMP	6.73 ± 1.89	65.29 ± 24.10	65.66 ± 29.73	0.57
Spruce BKP	3.80 ± 1.47	38.49 ± 14.60	44.96 ± 17.24	16.81

SD: Standard deviation

LM: freespan length was measured with Leica DM4500 light microscope and LCS software (Leica) under incidental light mode. 20 × lens

Simple size: 15

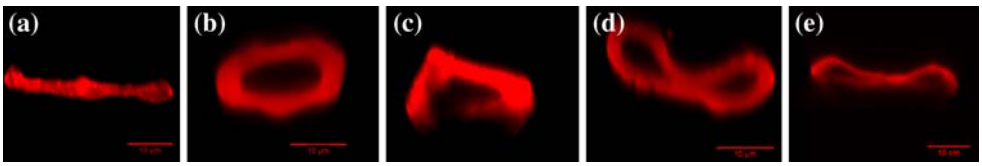

Fig. 8 Cross section views of fibers with CLSM operating in *YZ* scanning mode. (**a**) Spruce BKP without wet pressing; (**b**) Birch BCTMP without wet pressing; (**c**) Birch BCTMP after wet pressing; (**d**) Aspen BCTMP without pressing; (**e**) Aspen BCTMP after wet pressing

Table 3 Fiber collapsibility and fiber-wall elastic moduli calculated from the fiber cross sectional dimensions

Pulp Sample Type	Fiber wall thickness	Aspect ratio of un-pressed fibers	Aspect ratio of fibers pressed @340 kPa	Moment of inertia of compressed fibers, $I \times 10^{22}$ m^4	Elastic modulus E** (GPa)
Spruce BKP*	1.36 ± 0.44	10.18 ± 3.29	10.74 ± 3.50	0.95	1.43
Aspen BCTMP	2.39 ± 0.48	1.84 ± 0.47	3.76 ± 0.87	6.54	2.27
Aspen CTMP	2.24 ± 0.57	1.37 ± 0.25	3.06 ± 0.54	10.65	17.17
Birch CTMP			2.42 ± 0.83	24.51	2.53
Birch BCTMP	3.09 ± 0.79	1.25 ± 0.25	2.42 ± 0.83	24.51	2.38
LCR	–	–	3.85 ± 1.08	7.51	0.56
MCR	–	–	3.53 ± 0.69	6.59	0.22

* Pressed at 220 kPa

** E was calculated from the flexibility *(F)* and moment of inertia *(I)* according to Eq. 3

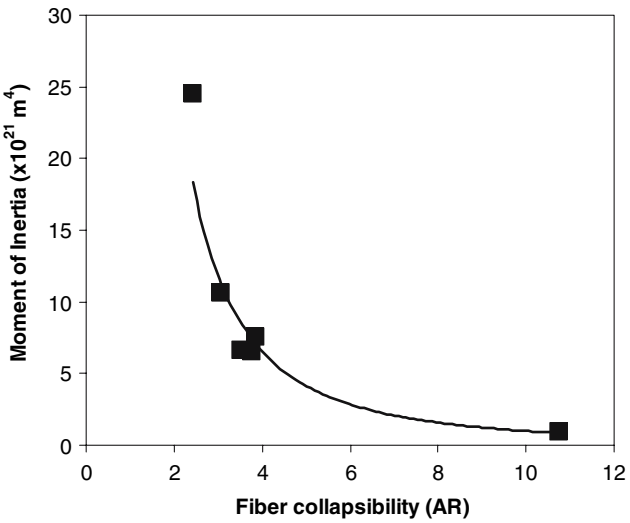

Fig. 9 Effect of fiber collapsibility on moment of inertia of fiber

pressing. The thick-walled birch fibers collapse partially even after pressing. Figure 10 illustrates how the fiber wall thickness affects the fiber collapsibility (*AR*) and in turn, affects the fiber moment of inertia.

Fiber-wall modulus

With CLSM, the moment of inertia can be calculated with Eq. 3. This made it possible to measure the longitudinal elastic modulus of the fiber wall. It can be seen from Table 3 that the elastic modulus obtained in this study is in the range of 1.4–17.2 GPa for the softwood BKP and hardwood BCTMP. The result is comparable to the elastic modulus of wet pulp fibers obtained with micro-tensile test, which is of the order of 10 GPa [22, 29]. For spruce BKP, the measured elastic modulus of 1.4 GPa is slightly lower than 4.3 GPa reported by Ehrnrooth [29]. In addition to the difference in the types of fibers, the contribution of shear deformation to measured flexibility may lead to a lower *E,* calculated from Eq. 3 due to the pure bending assumption, according to Waterhouse and Page [22].

Both bleaching and refining altered the elastic modulus of the fiber wall significantly (Table 3). The elastic modulus of aspen CTMP has been reduced from 17.2 to 2.3 GPa by bleaching, and is then further reduced to 0.6 and 0.2 GPa by LC refining and MC refining, respectively. It is interesting to find that the fiber collapsibility is not much affected by the elastic modules. As shown in Fig. 11a, different aspen fibers have almost the same *AR,* but completely different *E*, from 0.2 to 17.2 GPa. This, on the other hand, further confirms that fiber wall thickness is the predominant factor in determining the fiber collapsibility. According to Eq 3, the fiber flexibility relates linearly to the reciprocal of elastic modulus; however, there is certain discrepancy between the theory and the experimental results as shown in Fig. 11b. This may be partially due to the shear contribution to the overall bending as

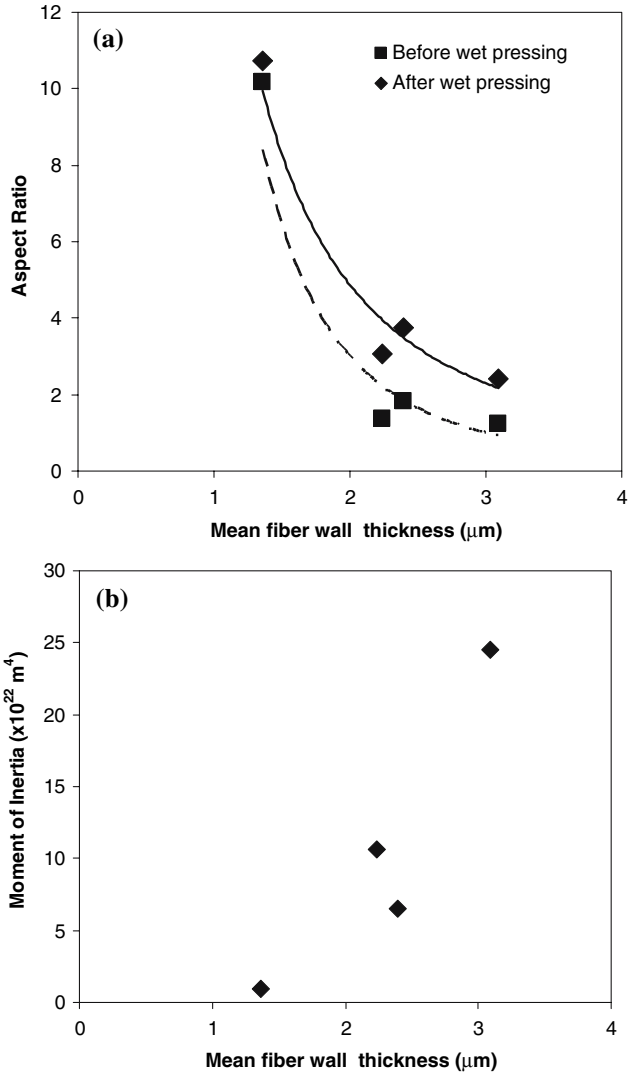

Fig. 10 Effect of fiber wall thickness on fiber collapsibility (**a**) and moment of inertia (**b**)

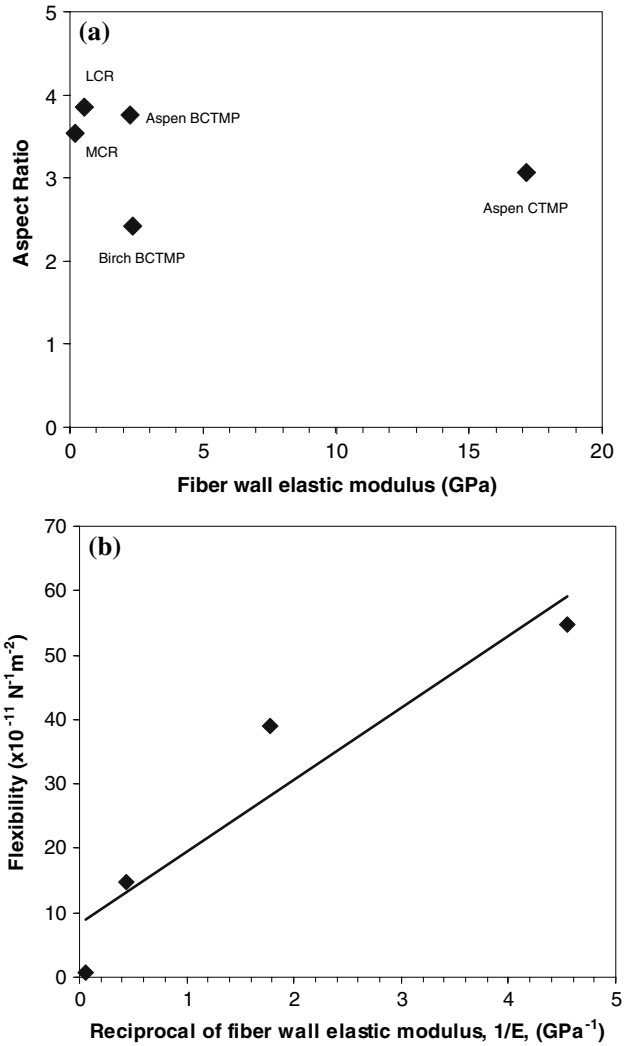

Fig. 11 Effect of fiber wall elastic modulus on fiber collapsibility (**a**) and flexibility (**b**)

discussed forgoing, since Eq. 3 only considers pure bending.

In general, collapsed fibers are more flexible as shown in Fig. 12. For aspen fibers, the flexibility is mainly determined by the elastic modulus, and the collapsibility has little effect since it does not change much. Bleaching and mechanical treatment slightly altered the collapsibility, but significantly improved the flexibility. This new understanding may have significant impact on the use of BCTMP fibers in wood-free fiber paper grades and multi-ply board grades. In both cases, the major objective is to increase paper bulk by adding BCTMP fibers in the furnish. However, adding too much BCTMP may reduce the paper strength. Bleaching does not increase the fiber collapsibility, which means paper bulk can be maintained, but bleaching can increase fiber flexibility by decreasing the elastic modulus of the fiber wall, thus increasing the bonded area among fibers. Therefore, the manufacturer may adjust the pulp properties by modifying the bleaching process in BCTMP manufacturing.

Accounting for the measured flexibility values

The flexibility of birch and aspen CTMP and BCTMP fibers are in the range of 0.7×10^{11}–14.8×10^{11} N^{-1} m^{-2}. As compared to the flexibility values of softwood mechanical fibers obtained by hydrodynamic method [5, 10, 30], which are in the range of 0.1×10^{11}–0.4×10^{11} N^{-1} m^{-2}, the CLSM method obtained much higher values. But it is comparable to the flexibility of spruce TMP fibers obtained by the Steadman method, which is 3.8×10^{11}–16.0×10^{11} N^{-1} m^{-2} [13]. First, the sample fibers are not the same although they are all mechanical pulp fibers. Second, in the conformability method, a wet pressing was

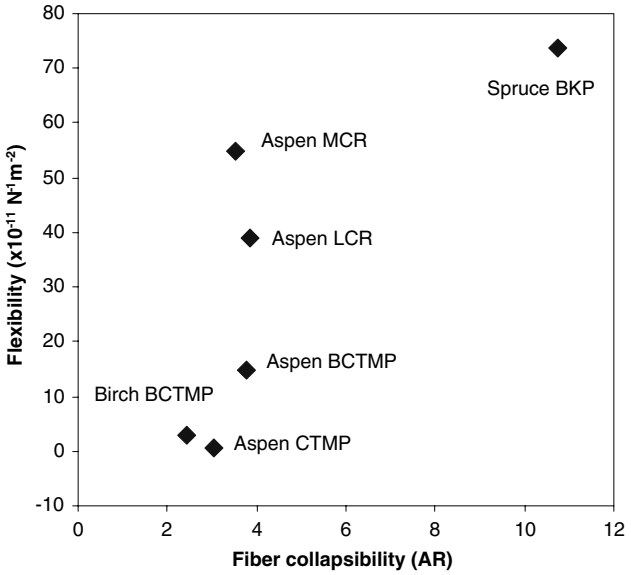

Fig. 12 Relationship between measured fiber flexibility and collapsibility

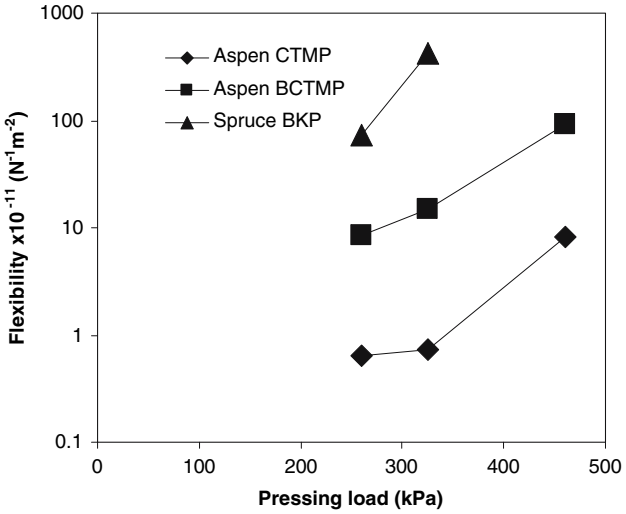

Fig. 13 Effect of wet pressing on measured flexibility values

conducted before measuring the flexibility. In the hydrodynamic methods, fiber deformation is caused by hydrodynamic forces which do not cause fiber collapse. Third, hydrodynamic methods only measure fiber bending flexibility, whereas the conformability method includes both shear and bending contributions [22]. As discussed previously, collapsibility substantially affects the measured flexibility value with the Steadman method. Therefore, the wet pressing, which causes fiber collapse before the flexibility measurement, will affect the measured flexibility value. Figure 13 shows the relationship between the pressure used in the wet pressing and the measured flexibility results. It can be seen that by increasing pressure load, flexibility for all the three types of fibers increases. Since flexibility greatly depends on the collapsibility of the fibers, and in the papermaking process fibers are wet pressed, the flexibility measured with the Steadman method may be more representative of the fiber flexibility in the papermaking process.

The measured flexibility, 73.7×10^{11} N^{-1} m^{-2}, of bleached spruce Kraft fibers is also much higher than that of 1.8×10^{11} N^{-1} m^{-2} for unbeaten black spruce Kraft fiber by the hydrodynamic method [6]. According to Waterhouse and Page [22], shear is a major part of the deformation in the Steadman method for collapsed and flexible fibers. As shown foregoing in Fig. 5a, the BKP fibers yield a span composed of two straight line segments, which features the shear deformation. Therefore, the larger flexibility value measured with the Steadman method may be due to the inclusion of the Shear deformation. The flexibility of unbleached spruce kraft fibers, 22.4×10^{11} N^{-1} m^{-2}, obtained by Karnis [13] with the Steadman method is also lower than that of bleached spruce BKP measured in this study. The elastic modulus of cell wall may be changed in bleaching, which leads to a higher fiber flexibility. In addition, the difference in measured freespan length with CLSM and LM, as discussed before, may also need to be taken into consideration.

Conclusions

A new method for measuring the flexibility of individual wet fibers has been developed using CLSM and image processing on the basis of Steadman and Luner method. With CLSM, the freespan length and the deflection height can be directly determined from the fiber transverse view of the fiber span. A neutral bending plane was defined, which gives more accurate measurement of the freespan length. The difference in freespan length measured with CLSM and LM was as much as 25%. From the transverse view of the fiber span, the features of shear deformation and bending deformation can be revealed. With CLSM optical sectioning function, the cross-sectional view of a fiber can be obtained, which can be used to determine the collapsibility of fibers before the flexibility measurement. In addition, the moment of inertia of fibers can be calculated from the dimension of fiber cross section. Therefore the elastic modulus of fiber walls can be calculated from the measured flexibility.

Results show that the collapsibility of fibers greatly affects the measured flexibility values. Collapsed fibers are more flexible due to the reduced fiber cross section area or moment of inertia. The collapsibility is mainly determined by the fiber wall thickness. The contribution of fiber wall elastic longitudinal modulus is minimal. Fiber flexibility is also affected by the elastic modulus of the fiber wall. Both

a bleaching process and a refining process can significantly reduce the elastic modulus of the fiber wall, thereby increasing the fiber flexibility.

With this CLSM method, image processing software can be used for the measurement, so that the subjective errors are avoided. More importantly, when the flexibility is measured, fiber collapsibility, and fiber wall elastic modulus can also be determined, which leads to more fundamental understanding of the factors affecting fiber flexibility. This will also shed light on how to modify the pulp and paper process to obtain desirable fiber flexibility.

Acknowledgements The authors would like to acknowledge the financial support of Atlantic Innovation Fund (AIF), Canadian Foundation for Innovation (CFI), and New Brunswick Innovation Fund (NBIF) to this research work.

References

1. Nilsson B, Lars W, Gray D (2001) 12th Fundamental Research Symposium, p 211
2. Jang HF (2001) 12th Fundamental Research Symposium, p 193
3. Samuelsson LG (1963) Svensk Papperstidn 15(1):S41–S46
4. Mohlin U-K (1975) Svensk Papperstidn 78(11):412–416
5. Kerekes RJ, Tam Doo PA (1985) J Pulp Paper Sci 11:60–61
6. Kuhn DCS, Lu X, Olson JA, Robertson AG (1995) J Pulp Paper Sci 21(1):337
7. Steadman R, Luner P (1981) 8th Fundamental Research Symposium, p 211
8. Seborg CO, Simmonds FA (1941) Paper Trade J 113(1):49–50
9. James WL (1973) Wood Sci 6(1):30–38
10. Tam Doo PA, Kerekes RJ (1981) Tappi 64:113–116
11. Zhang M, Hubbe MA, Venditti RA, Heitmann JA (2004) J Pulp Paper Sci 30:29–34
12. Delgado E, Lopez-Dellamary FA, Allan GG, Andrade A, Contreras H, Regla H, Cresson T (2004) J Pulp Paper Sci 30:141–144
13. Karnis A (1994) J Pulp Paper Sci 20(1):280–288
14. Lawryshyn YA, Kuhn DCS (1996) J Pulp Paper Sci 22(1):423–431
15. Lowe R, Ragauskas A, Page DH (2005) Imaging fibre deformations. In: I'Anson SJ (ed) Advances in paper science and technology, Proc. 13th Fundamental Research Symposium. FRC, Manchester, pp 921
16. Jang HF, Howard RC, Seth RS (1995) Tappi J 78(1):131
17. Jang HF, Amiri R, Seth RS, Karnis A (1996) Tappi J 79:203
18. Jang HF, Seth RS, Wu CB, Chan BK (2003) Determining the transverse dimensions of fibres in wood using confocal microscopy. In International Paper Physics Conference, Victoria, BC, Canada, p 313
19. Jang HF, Seth RS (1998) Tappi J 81:167–174
20. Ozaki Y, Bousfield DW, Shaler SM (2005) J Pulp Paper Sci 31:48–52
21. Li K, Reeve DW (2005) Cellulose Chem Technol 39(3):211–223
22. Waterhouse JF, Page DH (2004) Nordic Pulp Paper Res J 19:89–92
23. The Mathworks Inc (2004) Matlab Reference Manuel
24. Otsu N (1979) IEEE Trans Syst Man and Cybern SMC-9:62–66
25. Haralick RM, Linda GS (1992) Computer and robot vision. Addison-Wesley
26. Jang HF, Seth RS (1998) Characterization of the collapse behaviour of papermaking fibres using confocal microscopy. In the Proceedings of the 84th Annual Meeting of the Technical Section of Canadian Pulp and Paper Association, p 205
27. Mark RE (2002) Handbook of physical testing of paper II. Marcel Dekker, NY
28. Jang HF, Robertson AG, Seth RS (1992) Measuring fibre coarseness and wall thickness distributions with confocal microscopy. In the Proceedings of 78th Annual Meeting of the Canadian Pulp and Paper Association, Montreal, Que, Canada, p 189
29. Ehrnrooth EML, Kolseth P (1984) Wood fibre Sci 16(4):549–566
30. Tam Doo PA, Kerekes RJ (1982) Pulp Pap Can 83(2):46–50